Fuel 321 (2022) 123957

Contents lists available at ScienceDirect

Fuel

journal homepage: www.elsevier.com/locate/fuel

Full Length Article

Reduced graphene oxide improves the performance of a methanogenic biocathode

D. Carrillo-Peña [a], R. Mateos [a], A. Morán [a], A. Escapa [a,b,*]

[a] Chemical and Environmental Bioprocess Engineering Group, Natural Resources Institute, University of León, León 24071, Spain
[b] Department of Electrical Engineering and Automatic Systems, University of León, León 24071, Spain

ARTICLE INFO

Keywords:
Biocathode
Carbon dioxide
Electromethanogenesis
Graphene oxide
Microbial electrosynthesis

ABSTRACT

Microbial electrosynthesis (MES), a sub-branch of bioelectrochemical processes, takes advantage of a certain type of electroactive microorganism to produce added value products (such as methane) from carbon dioxide (CO_2). The aim of this study is to quantify the benefits of using a carbon felt electrode modified with reduced graphene-oxide (rgoCF) as a methanogenic biocathode. The current density generated by the rgoCF was almost 30% higher than in the control carbon felt electrode (CF). In addition, charge transfer and ohmic resistances were, on average, 50% lower in the rgoCF electrode. These improvements were accompanied by a larger presence of bacteria (31% larger) and archaea (18% larger) in the rgoCF electrode. The microbial communities were dominated by hydrogenotrophic methanogenic archaea (*Methanobacterium*) and, to a lesser extent, by a low-diversity group of bacteria in both biocathodes. Finally, it was estimated that for a CO_2 feeding rate in the range 15–30 g CO_2 per m^2 of electrode per day, it is possible to produce a high-quality biogas (>95% methane concentration).

1. Introduction

Thanks to their ability of using wastes as fuel feedstock, bio-electrochemical systems (BES) can potentially become a sustainable technology capable of providing energy-related goods and services with a low environmental footprint. BES can be seen as electrochemical systems in which at least one of the electrode reactions is catalyzed by electroactive microorganisms. This catalysis involves complex biological processes that culminate in the release or acceptance of electrons to/from a solid surface (electrode) [1]. Similar to other electrochemical systems, BES are reversible and can operate in galvanostatic (in this case BES are usually referred to as microbial fuel cells, or MFC) or electrolytic mode (usually referred to as microbial electrolysis cells, MEC) [2]. When the latter uses CO_2 as a feedstock to produce organic compounds it is referred to as microbial electrosynthesis (MES), and if the end product is methane many researchers refer to it as electromethanogenesis (EM) [3]. This paper focuses precisely on the latter and for more detailed information on BES and EM, the reader is referred elsewhere [4-6].

The topography and chemistry of the electrode surface affects not only the formation and structure of the electroactive biofilm, but also the electron transfer processes taking place between electrodes and microorganisms [7]. As a result to that, there is a large body of literature dealing with different methods and approaches to modify the electrodes surface [7]. These modifications are usually undertaken at the nano-, micro- or macro-scale [7,8]. Modification at the nano-scale usually seek an intimate electrical interaction between the electroactive biofilm and the electrodes [7,9-12]. In this regard, graphene and its derivatives have received notable interest in the past few years, as they can provide bioelectrodes with high electrical conductivity, increased surface area, and enhanced electrocatalytic activity and chemical stability [7,13]. As a result, the use of graphene on bioanodes has been largely investigated, revealing that it can greatly improve their performance [13-15]. For instance, Roubaud *et al.* [14] reported that modifying the nano-topography of bioanodes with graphene oxide resulted in a better attachment of bacteria and a larger surface area. In another study it was found that the use of graphene-modified bioanodes reduced the start-up time, compared to the control electrode, acting as a selective agent for exoelectrogenic bacteria such as *Geobacter* [13]. In addition, Sayed *et al.* [15] observed that graphene oxide enhanced the electron transfer rate, resulting in an up to 10-fold improvement in current density.

In contrast to bioanodes, only a few papers have investigated the benefits of using graphene on biocathodes [16-23]. Hu et al. [18]

* Corresponding author at: Department of Electrical Engineering and Automatic Systems, University of León, León 24071, Spain.
E-mail address: adrian.escapa@unileon.es (A. Escapa).

https://doi.org/10.1016/j.fuel.2022.123957
Received 23 July 2021; Received in revised form 16 February 2022; Accepted 20 March 2022
Available online 8 April 2022

developed a graphene-modified carbon-felt electrode for microbial electroreduction of CO_2 to fatty acids. They found that the presence of graphene resulted in higher current densities and enhanced acetate and butyrate production efficiencies. Aryal et al. [21] used a carbon felt cathode, coated with three-dimensional graphene to transfer electrons to a pure culture (*Sporomusa ovata*) capable of reducing CO_2 to acetate, while significantly improving electrical current and chemical production rates. In another study, it was found that biocompatible copper electrodes coated with graphene oxide promoted the formation of a dense, electroactive biofilm, while the uncoated copper electrodes were only covered by scattered and damaged cells [22]. These studies demonstrate that graphene can be used as an excellent conductor with electrochemical properties that enable high-performance microbial electrosynthesis [21,22]. However, and to the authors' knowledge, none of them have explored the impact of graphene on methane-producing biocathodes. Thus, in this paper we aim to quantify the benefits of using a graphene-modified biocathode to produce methane from CO_2. This quantification is made in terms of productivity, electrochemical performance and the structure of the electroactive biofilm formed on the surface of the electrode.

2. Materials and methods

2.1. Preparation of graphene oxide-modified electrode

Graphene oxide (GO; 4 mg·mL, dispersion in H_2O, SIGMA-ALDRICH Chemie GmbH, Germany) was electrodeposited on two carbon felt electrodes (soft felt SIGRATHERM GDF-2, SGL Carbon Group, Wiesbaden, Germany) with a total projected surface area of 7.5 cm^2 each. The electrodeposition process was carried out in an oxygen-free environment (nitrogen bubbling) through a series of 16 cyclic voltammetries at a scan rate of 20 $mV{\cdot}s^{-1}$ and a voltage range between −1.5 V and 0.8 V versus Ag/AgCl (3 M). The minimum potential selected to perform the simultaneous reduction-electrodeposition process (-1.5 V) was selected according to [24]. A platinum wire mesh (2 cm × 2 cm, Goodfellow, UK) was used as a counter electrode (CE) and an Ag/AgCl 3 M KCl, as a reference electrode (RE). The electrolyte consisted of an aqueous solution containing 150 mM NaCl and 0.5 $mg{\cdot}mL^{-1}$ of GO (TheGrapheneBox, Spain). The solution was previously neutralized with 0.5 M KOH and then sonicated for 15 min. The CV profiles obtained during the electrodeposition process are shown in the supplementary information (Figure S1a). To confirm rGO electrodeposition, CVs were performed on both CF and rgoCF at a scan rate of 5 $mV{\cdot}s^{-1}$ in a solution containing 3.4 mM $K_3Fe(CN)_6$ and 0.1 M KCl as the supporting electrolyte (see Figure S1b). The resulting voltammograms displayed higher peaks and a much smaller peak-to-peak separation on the rgoCF, all of which indicates a higher electrocatalytic activity and a closer behavior to reversibility of the modified electrode, thus confirming the electrodeposition of rGO on the rgoCF electrode [13].

2.2. Setup. Bioreactor construction and operational conditions

The experiments were carried out in a two-chamber H-cell reactor type that consisted of two identical 500 mL glass bottles (ADAMS & CHITTENDEN, Scientific glass) separated by a cation exchange membrane (Fig. 1). The cathode (working electrode) consisted of four carbon-felt pieces (1.5 cm × 1.5 cm × 0.5 cm) connected to titanium wires partially coated with an insulating material to prevent electrical contact between them. Two of them were electrodeposited with GO (they will be referred to as rgoCF throughout the manuscript) following the method described above. The other two were unmodified carbon felt (they will be referred to as CF throughout the manuscript). All cathodes were pretreated, as described in [25]. The anode (counter electrode) consisted of a platinum wire mesh (2 cm × 2 cm, Goodfellow, UK). An Ag/AgCl reference electrode was placed in the cathode chamber in the vicinity of the working electrodes. The biocathode potential was set to −1 V vs Ag/AgCl using a Biologic multichannel potentiostat (EC lab software, version 11.31) in a three-electrode configuration. The cell was kept inside a thermal chamber (Fitotron, SANYO) that maintained the temperature at 30 ± 0.5 °C, and it was operated in batch mode. In addition, it was stirred at 200 rpm (Magnetic stirrer plate IKA-WERKE RO 15, Germany) to enable mixing and to facilitate mass transfer inside the cathode chamber.

2.3. Inoculum, growth media and experimental phase

The effluent from the cathodic chamber of a CH_4-producing microbial electrosynthesis cell that was operated for approximately 200 days

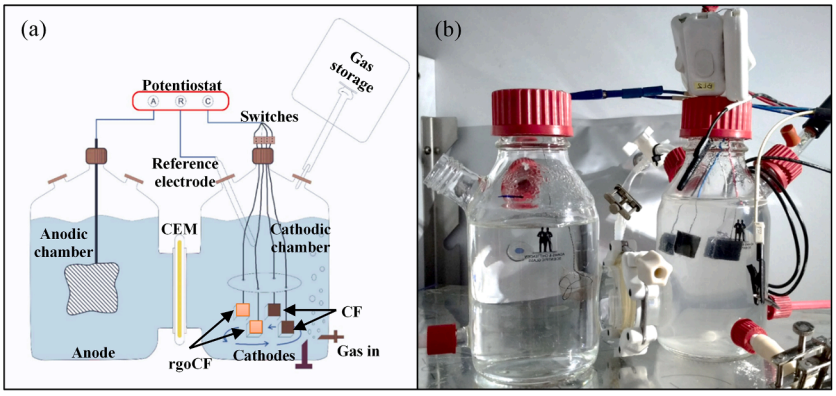

Fig. 1. Microbial electrosynthesis reactor (H-Cell MES): (a) reactor configuration and (b) actual reactor assembly.

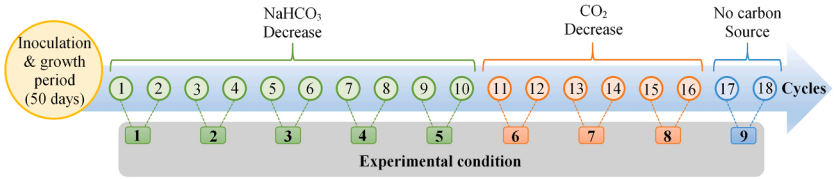

Fig. 2. Experimental timeline.

in our laboratory [26] was used as inoculum. The cathode chamber was filled with 250 mL of effluent, 250 mL of medium, 5 $g \cdot L^{-1}$ $NaHCO_3$, 200 mL of CO_2 and 200 mL of hydrogen in the inoculation phase. The medium contained: 3.21 g K_2HPO_4, 1.57 g KH_2PO_4, 0.01 g $CaCl_2$, 0.09 g $MgCl_2$, 0.01 g $MgSO_4$, and 0.28 g NH_4Cl (pH 7.1). 1 mL of mineral solution and 1 mL of vitamin solution was used per litre [27]. The anode chamber was filled with 500 mL of medium without vitamin solution, to avoid the growth of microorganisms. Before inoculation, the headspace of the cathode chamber was flushed with N_2 gas for 30 min. Following inoculation, and after 10 cycles of batch operation (50 days), the current stabilized in both CF and rgoCF electrodes (Figure S2). Afterwards, the experimental phase began (Fig. 2). It consisted of 18 batch cycles (4–5 days duration) where the concentration of the carbon source was progressively reduced. Each concentration was maintained for two cycles, which resulted in nine different experimental conditions (2 cycles per condition). From conditions 1 to 5, the concentration of $NaHCO_3$ was gradually reduced to zero, keeping CO_2 constant. From conditions 6 to 8, the CO_2 concentration was again gradually decreased and finally, in the last test no carbon source was fed.

2.4. Bioelectrochemical operation and electroanalytical characterization

A biologic VSP potentiostat was used to run simultaneous multitechnique electrochemical routines with the EC-Lab software v.11.31, which included chronoamperometry (CA), cyclic voltammetry (CV) and electrochemical impedance spectroscopy (EIS). During the chronoamperometry tests, the cathode was polarized at −1 V (vs. Ag/AgCl – 3 M KCl) and current production was monitored every 120 s.

CVs (scan rate of 5 $mV \cdot s^{-1}$) and EIS (frequency range of 10^5 to 10^{-2} Hz) analyses were performed before inoculation and at the end of each cycle.

Volatile fatty acids (from C2 to C6) were analyzed using a gas chromatograph (Bruker 450-GC) with a flame ionization detector (FID). Total organic carbon (TOC), total inorganic carbon (IC) and total nitrogen (TN) were measured using an analyzer (multi N/C 3100, Analytikjena). Dissolved oxygen (Hach, HQ40d - two-channel digit multimeter), redox (pH-Meter, pH 91; Wissenschaftlich Technische Werkstätten, WTW) and pH (pH-Meter BASIC 20+, Crison) measurements were performed following standard methodologies. A gas chromatograph (Varian CP3800 GC) equipped with a thermal conductivity detector (TCD), determined the composition of the gas in terms of hydrogen (H_2), carbon dioxide (CO_2), oxygen (O_2), nitrogen (N_2) and methane (CH_4).

2.5. Extraction of DNA and microbial community structure determination

The biocathodes were cut into samples of about 300 mg of electrode. These samples were used to characterize the microorganism that had developed at the methane-producing biocathode at the end of the experiment (cycle 18). Microbial communities were analyzed and followed along the experimental time by high throughput sequencing of massive 16S rRNA gene libraries. Total bacteria and archaea were analyzed. Genomic DNA was extracted with a DNeasy PowerSoil Kit (Qiagen) according to the manufacturer's instructions. All PCR reactions were carried out in a Mastercycler (Eppendorf, Hamburg, Germany), and PCR samples were checked for the size of the product on a 1% agarose gel and quantified by a NanoDrop 1000 (Thermo Scientific). The entire DNA extract was used for high-throughput sequencing of 16S rRNA gene-based libraries with 16S rRNA gene-based primers for Bacteria 27Fmod −519R and for Archaea 349F-806R. The Novogene Company (Cambridge, UK) carried out Illumina sequencing using a HiSeq 2500 PE250 platform.

The obtained DNA readings were compiled in FASTq files for further bioinformatics processing, carried out using QIIME software, version 1.7.0 [28]. Sequence analysis was performed by the Uparse software (v7.0.1001) using all the effective tags. Sequences with $\geq$ 97% similarity were assigned to the same OTUs. The representative sequence for each OTU was screened for further annotation. For each representative sequence, Mothur software was used against the SSUrRNA database of the SILVA Database [29], for species annotation at each taxonomic rank (Threshold:0.8 ~ 1).

The quantitative analysis of all samples was analyzed by means of quantitative-PCR reaction (qPCR) using PowerUp SYBR Green Master Mix (Applied Biosystems) in a StepOnePlus Real-Time PCR System (Applied Biosystems). The qPCR amplification was performed for the 16S rRNA gene, in order to quantify the entire eubacteria community and for the mcrA gene, to quantify the total methanogen community. The primer set 314F qPCR (5′-CCTACGGGAGGCAGCAG-3) and 518R qPCR (5′-ATTACCGCGGCTGCTGG-3′) at an annealing temperature of 60 °C for 30 s was used for Bacteria and Arc 349F (5′-GYGCASCAGKCGMGAAW-3′) and Arc 806R (5′-GGACTACVSGGGTATCTAAT-3′) for Archaea quantification.

3. Results and discussion

To ensure that the two reduced graphene oxide-treated electrodes (rgoCF) and the two unmodified electrodes (CF) were exposed to the same operational conditions (i.e.: the same inoculum, temperature, pH, etc.), they were all immersed within the same catholyte (Fig. 1). Following inoculation, the electrodes were operated in batch mode (4–5 days duration for each batch cycle) along 10 consecutive cycles to favor the development of a stable electroactive biofilm on the cathodes. During the last three cycles, the averaged current density fluctuated in a range between 10 and 20% (Figure S2), so it was assumed that the biofilms were mature and stable enough to initiate the experimental period (the averaged current density tended to stabilize at around 1.2 $A \cdot m^{-2}$ in rgoCF and 0.6 $A \cdot m^{-2}$ in CF).

3.1. Current generation and CH_4 production at different feed concentrations

Typically, MES and EM experiments are carried out with an excess of CO_2, that leads to an unnecessary waste of this gas, and usually results in the production of a poor-quality biogas that contains large amounts of CO_2. Therefore, the first set of experiments was aimed at determining the optimal amount of inorganic carbon (both CO_2 and $NaHCO_3$) that must be fed to an EM reactor in order to maximize the amount of CH_4 in the biogas.

Fig. 3 summarizes the impact that a gradual reduction of inorganic carbon fed to the cell (Fig. 3a) had on current density (Fig. 3b) and biogas composition (Fig. 3c). Gradually reducing the amount of $NaHCO_3$ fed to the reactor (tests 1 to 6 in Fig. 3a) did not show any apparent influence on the averaged current density nor on the biogas quality, leading us to conclude that in the presence of excess CO_2, bicarbonate does not play any significant role on EM. However, reducing the amount of CO_2 (tests 7 to 9) resulted in an immediate decrease in current density and in a notable improvement in CH_4 richness in the biogas (~100%). The decrease in current can probably be attributed to an increase in pH (Figure S3), as the acidifying effect of CO_2 gradually disappears. A more direct link between current and CO_2 can safely be ruled out since at −1V

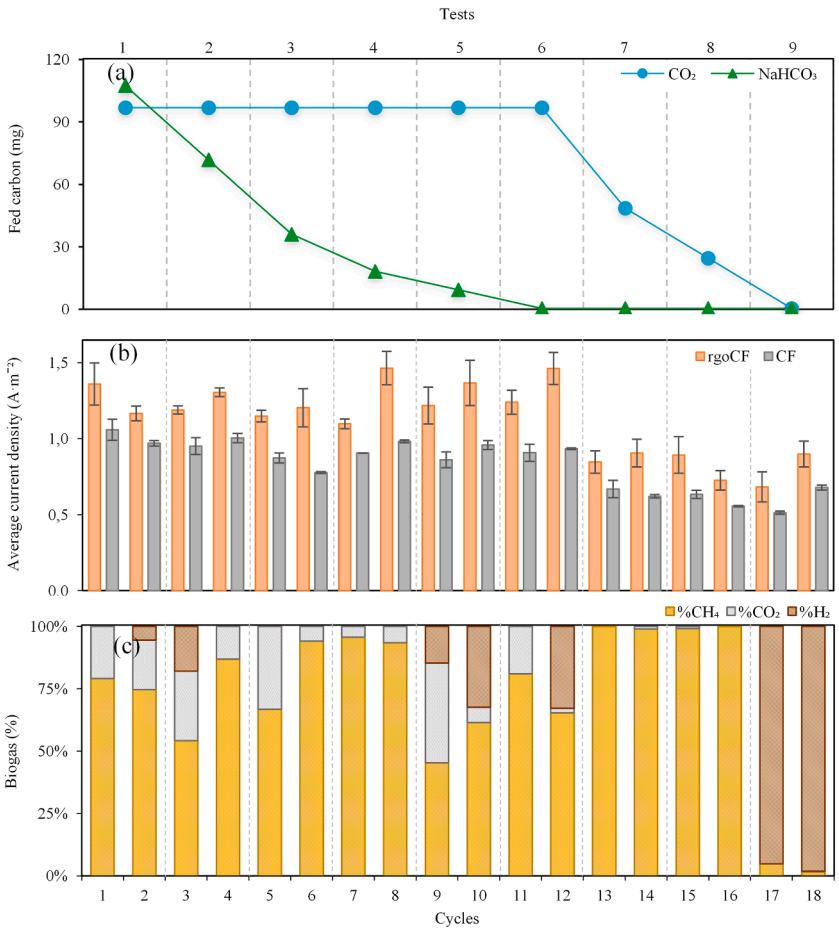

Fig. 3. Reactor evolution along cycles: (a) amount of inorganic carbon feed in terms of CO_2 gas and $NaHCO_3$, (b) average current density and (c) biogas composition.

vs Ag/AgCl CO_2, methanation occurs mainly through a two-step process, with hydrogen acting as an intermediary between current and CO_2 [30,31]. The fact that current is still being produced in the absence of CO_2 (test 9) supports this hypothesis.

It is noteworthy that, despite both electrodes showed a similar trend in current production, the rgoCF electrode generated approximately 58 ± 2% of the total current, while CF produced the remaining 42 ± 2% (Fig. 2b). This can likely be attributed to the presence of reduced graphene oxide on the rgoCF electrode, that induced lower ohmic and lower electron transfer over-potentials and favored the proliferation of electroactive microorganisms, as it will be shown in the following sections. Similar results were reported in [13] for bioanodes.

Regarding gas composition (Fig. 3c), it is important to emphasize that both electrodes are placed inside the same chamber (Fig. 1) and therefore, it is not possible to distinguish the individual contribution of any of them to CO_2 consumption and/or methane/hydrogen production. Still, the results from these experiments can provide a benchmark on the performance of an 'average EM biocathode'. In addition, and in contrast to current density (Fig. 3b), gas composition showed a quite erratic behavior through tests 1 to 6 (i.e. those tests where $NaHCO_3$ concentration was gradually reduced), which may indicate that the methanogenic activity (rather than the electrogenic activity) is the dominant source of variability in EM. For tests 7 and 8, when gaseous CO_2 was the only carbon source, methane concentration in the off-gas raised above 95%, indicating that our system cannot absorb CO_2 concentrations above 90 mg carbon·L^{-1}. Overall, it seems that in our set-up and with our operating conditions (for 4–5 days batch cycles duration and an electrode-surface-area to cathodic-chamber-volume ratio of 6 m^2 m^{-3}), the optimal CO_2 feed rate might be between 15 and 30 g of CO_2 per m^2 of electrode per day (g $CO_2 \cdot m^{-2} \cdot d^{-1}$). If we assume that the individual contributions of the two electrodes to CO_2 usage are proportional to current density, we can assume that the rgoCF electrodes might use up to 17–37 g $CO_2 \cdot m^{-2} \cdot d^{-1}$. Of course, this is a rough estimate for a sub-optimal, laboratory-scale EM system. In spite of that, and as mentioned above, these figures can provide a benchmark against which to compare future developments.

3.2. *Bioelectrochemical characterization of biocathodes*

To gain knowledge on the effect that reduced graphene oxide has on the electromethanogenesis process, CV and EIS tests were carried out throughout the experimental phase.

3.2.1. *Cyclic voltammetry tests*

Fig. 4 shows the results of the CV tests for both electrodes at the beginning of cycle 4 (both CO_2 and $NaHCO_3$ are present), cycle 12 (only CO_2 is present) and cycle 18 (in the absence of both CO_2 and $NaHCO_3$). An abiotic carbon felt electrode was also used as a control. The

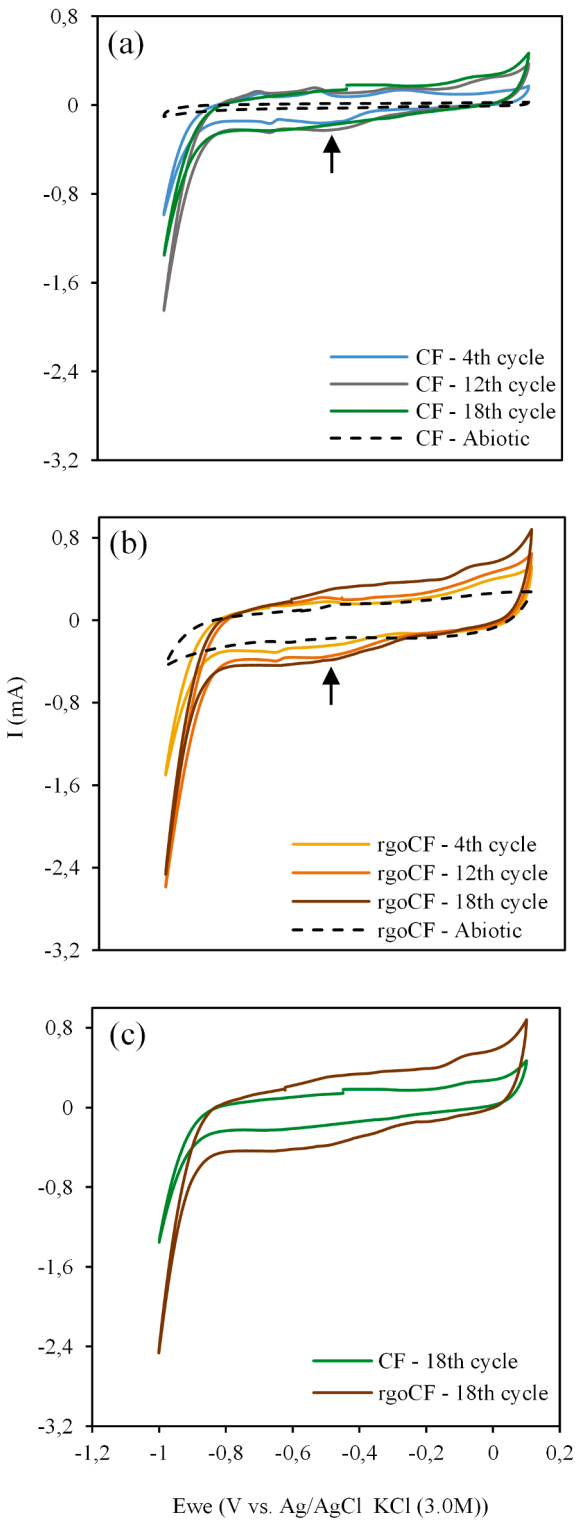

Fig. 4. Cyclic voltammetry of: (a) Abiotic and CF electrode over 3 different cycles, (b) Abiotic and rgoCF electrode over 3 different cycles and (c) CF and rgoCF electrode in cycle 18. Arrows indicate the peak corresponding to CO_2 direct reduction to CH_4.

voltammograms of rgoCF and CF exhibited the typical sigmoidal shape, displaying relatively high current densities (compared to the abiotic control electrode), which is indicative of the existence of well stablished electroactive biofilms [32]. In addition, both electrodes showed a reduction wave between −0.5 V and −0.6 V, which is consistent with the formal reduction potential of CO_2 to CH_4 ($CO_2 + 8H^+ + 8e^- \rightarrow CH_4 + 2H_2O$) under typical biological conditions (T = 25 °C, p = 1 bar, and pH 7.0) [33]. An additional wave appeared between −0.8 V and −1.0 V corresponding to the hydrogen evolution reaction (HER) under the same conditions [30]. The size of the peak associated with the HER in the CF electrode grew up to 1.8 mA on cycle 12, and fell to 1.3 mA on cycle 18. This represents a 27% reduction that might be related to an increase in pH, as discussed in Section 3.1. In contrast, the peak current of the HER in the rgoCF electrode did not show any decline with time and tended to stabilize at 2.4 mA after cycle 12. This seems to indicate that the rgoCF electrode is more robust to variations in the physicochemical conditions of the catholyte.

Another important feature is that the width of the voltammograms increases with time in both bioelectrodes, revealing a gradual increment of the electrical capacitance that can be directly linked to the development of a biofilm, as it will be shown in Section 3.2.2. The electrode pretreated with reduced graphene oxide presented a higher capacitance, something that has also been observed in bioanodes [13], and that might be relevant for short-term energy storage [3]. Finally, it is interesting to note that even in the absence of CO_2, the cathodic wave associated with CO_2 electroreduction to methane persists in the rgoCF electrode (cycle 18, Fig. 4c), while it practically disappears in the CF. We have not found any plausible explanation for this observation, and we can only hypothesize that the rgoCF electrode might have been accumulating small deposits of carbonates in previous cycles (probably as a result of local high pH) that were released when no CO_2 was feed to the electrode (cycles 17 and 18). The small amounts of CH_4 found in the off-gas in cycles 17 and 18 (Fig. 3c) would corroborate this hypothesis, although the question still remains why this does not occur in the CF electrode.

3.2.2. Electrochemical impedance spectroscopy (EIS)

At the beginning of cycle 12, and prior to the CV tests, the electrodes were subjected to EIS analyses (Fig. 5a) to gain a deeper knowledge of their electrochemical performance. It is common to analyze the EIS data by fitting them to an equivalent electrical circuit model that separates the individual contributions that electrochemical parameters have on the overall electrical impedance of the system [34]. In this study the EIS data (Fig. 5) was fitted to the circuit presented in the inset in Fig. 5b. This circuit consists of two electrical resistances: R_s, which comprises the sum of ohmic resistances of the electrode, the electrolyte and the contact resistance between the electrode and the current collector; and R_{ct}, that represents the charge transfer resistance. It also contains a capacitor (C) that models the biofilm and double-layer capacitance, and a Warburg impedance (W_d) related to diffusion phenomena. The parameters of the equivalent electrical circuit models of the three electrodes (CF, rgoCF and abiotic) are summarized in Table 1. R_S was significantly lower for the rgoCF electrode, which highlights the positive effect that reduced graphene oxide has on the surface conductivity of the electrode.

As expected, R_{ct} was distinctly larger in the abiotic electrode (Fig. 5a) [35]. Moreover, when comparing the two biotic electrodes, R_{ct} was>50 % lower in the rgoCF, indicating that the presence of reduced graphene oxide positively influences the electron transfer process. These results agree with the smaller over-potential of the hydrogen evolution reaction observed in the CV tests (Fig. 4c). Finally, the electrical capacitance of the rgoCF (531.3 μF) was twice as large as that of the CF (225.9 μF), and

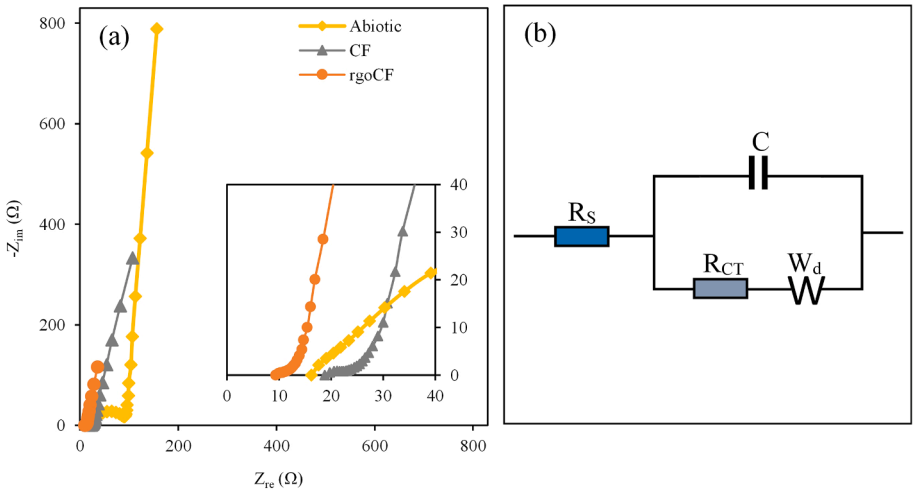

Fig. 5. (a) Nyquist plot comparing the abiotic electrode with the CF and rgoCF electrodes in cycle 12 (inset is an amplification of the high-frequency region) (b) electrical circuit used to fit the EIS data for Abiotic, CF and rgoCF electrodes.

Table 1
EIS fitting data for abiotic, CF and rgoCF electrodes in cycle 12.

	R_S	R_{CT}	C
Abiotic	20.7 Ω	52.3 Ω	14.5 μF
CF	21.6 Ω	5.4 Ω	225.9 μF
rgoCF	10.9 Ω	2.3 Ω	531.3 μF

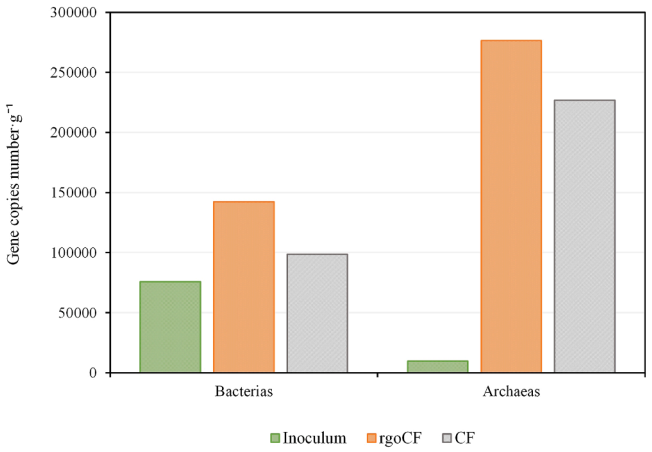

Fig. 6. Gene copies number in terms of Bacteria and Archaea in the inoculum, rgoCF and CF electrodes.

considerably larger than that of the abiotic electrode (14.5 μF), which again agrees with the results provided by the CV tests (Fig. 4c).

3.2.3. *Microbial community analysis*

Fig. 6 shows the quantifications (qPCR) of bacteria and archaea populations on the biofilms of the rgoCF and CF biocathodes. Both biofilms were dominated by methanogenic Archaea and, to a lesser extent, by a low-diversity group of Bacteria. The biofilm of the rgoCF electrode contained 31% more Bacteria and 18% more Archaea than the CF. This could be attributed to the fact that reduced graphene oxide accelerated the transference of electrons between species or from the electrode to the cells, which further improved the microbial growth [16].

The analysis of the microbial communities, in terms of Archaea and Bacteria, is shown in Fig. 7. The biocathodes were dominated by the *Methanobacterium* genus (family *Methanobacteriaceae*; phyla Euryarchaeota), representing > 99.8% in both cases. *Methanobacterium* is a hydrogenotrophic methanogen capable of producing CH_4 from CO_2 in the presence of H_2 as an electron donor [4,5], and it usually dominates methanogenic biocathodes [36,37].

Regarding bacteria, the biofilms of both electrodes contained families from the Proteobacteria (70–73%), Chloroflexi (11–16%), Firmicutes (5–6%) and Bacteroidetes (3–4%) phyla (see supplementary information, Figure S4), that are usually found in the biocathodes of MES and EM [38-41]. The phyla Chloroflexi, Bacteroidetes and Firmicutes (20–25%) are syntrophic assemblages of diverse bacteria that can ferment amino acids. However, the lack of any fermentative end-product in our system (total organic carbon analyses revealed a total absence of dissolved organic matter) indicates that, apparently, they are not playing any significant role, and their presence on the biocathodes may have originated from the inoculum [42].

The *Thiobacillus* genus, which was found in a relatively high abundance in our system (18–21%), might be helping to maintain the anaerobic conditions that are crucial for EM [40]. This hypothesis would be supported by previous studies that have reported the presence of *Thiobacillus* on the anodic chamber (anaerobic conditions) of microbial fuel cells [43], where it is expected to persist by consuming any intruding oxygen.

Hydrogen production can be explained by the presence of *Desulfovibrio* and *Geobacter,* two exoelectrogenic genera usually found in the biocathodes of EM and capable of catalyzing the hydrogen evolution reaction [4,44]. *Rhodocyclaceae*, an H_2-producing family [39] pertaining to the phylum of Proteobacteria, was also found in the biocathodes in proportions between 10 and 12% (Figure S5). However, no genera pertaining to this family were detected, as a result of their relative abundance at the genus level being below 1%.

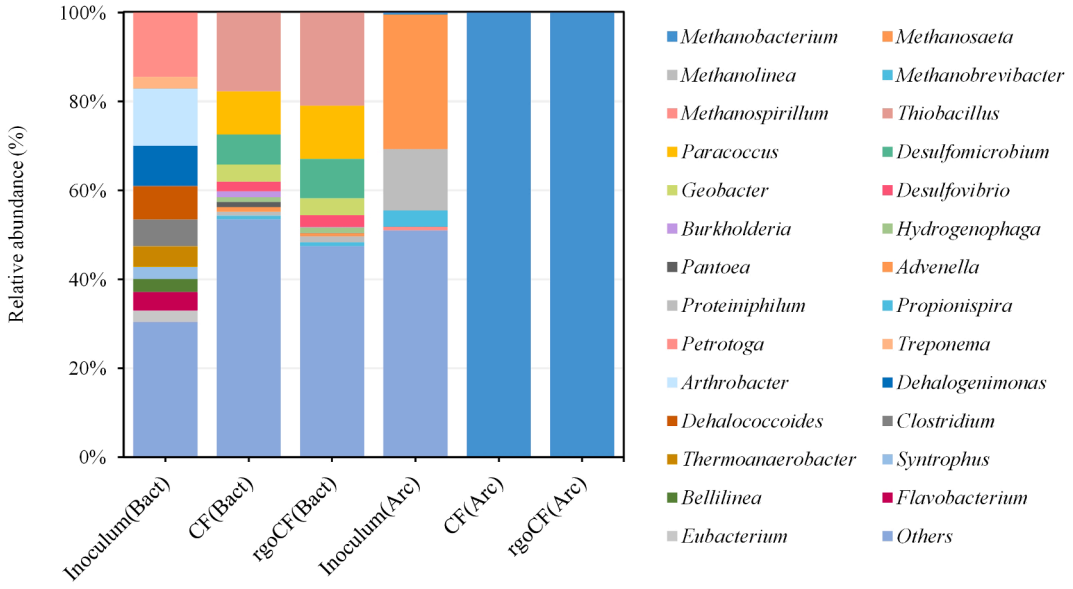

Fig. 7. Taxonomic classification of 16S rDNA Amplicon Sequencing gene from Bacteria and Archaea at genus level.

4. Conclusion

In this work we prove that methanogenic biocathodes pre-treated with reduced graphene oxide (rgo) can improve their bio-electrochemical activity and promote electromethanogenesis. The rgo-modified electrodes produced on average 38% more current that the unmodified ones, and the charge transfer and ohmic resistances were ~ 50% lower. The rgo-modified electrodes also promoted biofilm formation, resulting in 30% more Bacteria and 18 % more Archaea compared to unmodified electrodes. Finally, methane was mainly produced through the hydrogenotrophic route. Feeding CO_2 at a rate between 15 and 30 g $CO_2 \cdot m^{-2} \cdot d^{-1}$ allowed the production of a biogas with a methane richness higher than 95%. These results highlight the potential of this technology for practical application in areas such as biogas upgrading.

CRediT authorship contribution statement

D. Carrillo-Peña: Conceptualization, Investigation, Methodology, Writing – original draft. **R. Mateos:** Conceptualization, Investigation, Supervision, Methodology. **A. Morán:** Supervision, Writing – review & editing, Funding acquisition, Project administration. **A. Escapa:** Conceptualization, Supervision, Formal analysis, Writing – review & editing, Funding acquisition.

Declaration of Competing Interest

The authors declare that they have no known competing financial interests or personal relationships that could have appeared to influence the work reported in this paper.

Acknowledgments

This research was possible thanks to the financial support of the "Ministerio de Ciencia e Innovación (Gobierno de España)" project ref.: PID2020-115948RB-I00-TMA funded by MCIN/AEI/ 10.13039/ 501100011033, and the "Ente Regional de la Energía de Castilla y Leon" project ref.: EREN_2019_L3_ULE.

References

[1] Jadhav DA, Ghosh Ray S, Ghangrekar MM. Third generation in bio-electrochemical system research – A systematic review on mechanisms for recovery of valuable by-products from wastewater. Renew Sustain Energy Rev 2017;76:1022–31. https://doi.org/10.1016/j.rser.2017.03.096.

[2] Escapa A, Mateos R, Martínez EJ, Blanes J. Microbial electrolysis cells: An emerging technology for wastewater treatment and energy recovery. From laboratory to pilot plant and beyond. Renew Sustain Energy Rev 2016;55:942–56. https://doi.org/10.1016/j.rser.2015.11.029.

[3] Gomez Vidales A, Omanovic S, Tartakovsky B. Combined energy storage and methane bioelectrosynthesis from carbon dioxide in a microbial electrosynthesis system. Bioresour Technol Rep 2019;8:100302. https://doi.org/10.1016/j.biteb.2019.100302.

[4] Mateos R, Escapa A, San-Martín MI, de Wever H, Sotres A, Pant D. Long-term open circuit microbial electrosynthesis system promotes methanogenesis. J Energy Chem 2020;41:3–6. https://doi.org/10.1016/j.jechem.2019.04.020.

[5] Hara M, Onaka Y, Kobayashi H, Fu Q, Kawaguchi H, Vilcaez J, et al. Mechanism of electromethanogenic reduction of CO2 by a thermophilic methanogen. Energy Procedia 2013;37:7021–8.

[6] Mateos R, Escapa A, Vanbroekhoven K, Patil SA, Moran A, Pant D. Microbial electrochemical technologies for CO2 and its derived products valorization. Microb Electrochem Technol 2019:777–96. https://doi.org/10.1016/B978-0-444-64052-9.00032-7.

[7] Guo K, Prévoteau A, Patil SA, Rabaey K. Engineering electrodes for microbial electrocatalysis. Curr Opin Biotechnol 2015;33:149–56. https://doi.org/10.1016/j.copbio.2015.02.014.

[8] Saikia BK, Benoy SM, Bora M, Tamuly J, Pandey M, Bhattacharya D. A brief review on supercapacitor energy storage devices and utilization of natural carbon resources as their electrode materials. Fuel 2020;282:118796. https://doi.org/10.1016/J.FUEL.2020.118796.

[9] Zhao Y, Watanabe K, Nakamura R, Mori S, Liu H, Ishii K, et al. Three-dimensional conductive nanowire networks for maximizing anode performance in microbial fuel cells. Chem - A Eur J 2010;16(17):4982–5.

[10] Flexer V, Chen J, Donose BC, Sherrell P, Wallace GG, Keller J. The nanostructure of three-dimensional scaffolds enhances the current density of microbial bioelectrochemical systems. Energy Environ Sci 2013;6:1291–8. https://doi.org/10.1039/c3ee00052d.

[11] Jia X, He Z, Zhang X, Tian X. Carbon paper electrode modified with TiO2 nanowires enhancement bioelectricity generation in microbial fuel cell. Synth Met 2016;215:170–5. https://doi.org/10.1016/j.synthmet.2016.02.015.

[12] He Y-R, Xiao X, Li W-W, Sheng G-P, Yan F-F, Yu H-Q, et al. Enhanced electricity production from microbial fuel cells with plasma-modified carbon paper anode. PCCP 2012;14(28):9966. https://doi.org/10.1039/c2cp40873b.

[13] Alonso RM, San-Martín MI, Sotres A, Escapa A. Graphene oxide electrodeposited electrode enhances start-up and selective enrichment of exoelectrogens in bioelectrochemical systems. Sci Rep 2017;7. https://doi.org/10.1038/s41598-017-14200-7.

[14] Roubaud E, Lacroix R, Da Silva S, Esvan J, Etcheverry L, Bergel A, et al. Industrially scalable surface treatments to enhance the current density output from graphite bioanodes fuelled by real domestic wastewater. IScience 2021;24:102162. https://doi.org/10.1016/j.isci.2021.102162.

[15] Sayed ET, Alawadhi H, Olabi AG, Jamal A, Almahdi MS, Khalid J, et al. Electrophoretic deposition of graphene oxide on carbon brush as bioanode for microbial fuel cell operated with real wastewater. Int J Hydrogen Energy 2021;46(8):5975–83.

[16] Hu J, Zeng C, Liu G, Lu Y, Zhang R, Luo H. Enhanced sulfate reduction accompanied with electrically-conductive pili production in graphene oxide

modified biocathodes. Bioresour Technol 2019;282:425–32. https://doi.org/10.1016/j.biortech.2019.03.023.
[17] Su M, Wei L, Qiu Z, Jia Q, Shen J. A graphene modified biocathode for enhancing hydrogen production. RSC Adv 2015;5:32609–14. https://doi.org/10.1039/C5RA02695D.
[18] Hu N, Wang L, Liao MG, Liu K. Research on electrocatalytic reduction of CO2 by microorganisms with a graphene modified carbon felt. Int J Hydrogen Energy 2021;46:6180–7. https://doi.org/10.1016/j.ijhydene.2020.11.127.
[19] Annie Modestra J, Venkata MS. Capacitive biocathodes driving electrotrophy towards enhanced CO2 reduction for microbial electrosynthesis of fatty acids. Bioresour Technol 2019;294:122181. https://doi.org/10.1016/J.BIORTECH.2019.122181.
[20] Di Bari C, Goñi-Urtiaga A, Pita M, Shleev S, Toscano MD, Sainz R, et al. Fabrication of high surface area graphene electrodes with high performance towards enzymatic oxygen reduction. Electrochim Acta 2016;191:500–9.
[21] Aryal N, Halder A, Tremblay PL, Chi Q, Zhang T. Enhanced microbial electrosynthesis with three-dimensional graphene functionalized cathodes fabricated via solvothermal synthesis. Electrochim Acta 2016;217:117–22. https://doi.org/10.1016/j.electacta.2016.09.063.
[22] Aryal N, Wan L, Overgaard MH, Stoot AC, Chen Y, Tremblay P-L, et al. Increased carbon dioxide reduction to acetate in a microbial electrosynthesis reactor with a reduced graphene oxide-coated copper foam composite cathode. Bioelectrochemistry 2019;128:83–93.
[23] Dai H, Yang H, Liu X, Jian X, Liang Z. Electrochemical evaluation of nano-Mg(OH)2/graphene as a catalyst for hydrogen evolution in microbial electrolysis cell. Fuel 2016;174:251–6. https://doi.org/10.1016/J.FUEL.2016.02.013.
[24] Ambrosi A, Pumera M. Precise tuning of surface composition and electron-transfer properties of graphene oxide films through electroreduction. Chem - A Eur J 2013;19:4748–53. https://doi.org/10.1002/chem.201204226.
[25] Mateos R, Alonso R, Escapa A, Morán A. Methodology for fast and facile characterisation of carbon-based electrodes focused on bioelectrochemical systems development and scale up. Materials 2017;10(1):79.
[26] Pelaz G, Carrillo-Peña D, Morán A, Escapa A. Electromethanogenesis at medium-low temperatures: impact on performance and sources of variability. Fuel 2022;310:122336.
[27] Van Eerten-Jansen MCAA, Veldhoen AB, Plugge CM, Stams AJM, Buisman CJN, Ter Heijne A. Microbial community analysis of a methane-producing biocathode in a bioelectrochemical system. Archaea 2013;2013:1–12.
[28] Caporaso JG, Kuczynski J, Stombaugh J, Bittinger K, Bushman FD, Costello EK, et al. QIIME allows analysis of high-throughput community sequencing data. Nat Methods 2010;7(5):335–6.
[29] Wang Q, Garrity GM, Tiedje JM, Cole JR. Naïve Bayesian classifier for rapid assignment of rRNA sequences into the new bacterial taxonomy. Appl Environ Microbiol 2007;73:5261–7. https://doi.org/10.1128/AEM.00062-07.
[30] Rozendal RA, Jeremiasse AW, Hamelers HVM, Buisman CJN. Hydrogen production with a microbial biocathode. Environ Sci Technol 2008;42:629–34. https://doi.org/10.1021/es071720+.
[31] Sangeetha T, Guo Z, Liu W, Gao L, Wang L, Cui M, et al. Energy recovery evaluation in an up flow microbial electrolysis coupled anaerobic digestion (ME-AD) reactor: role of electrode positions and hydraulic retention times. Appl Energy 2017;206:1214–24.
[32] Li Z, Fu Q, Kobayashi H, Xiao S, Li J, Zhang L, et al. Polarity reversal facilitates the development of biocathodes in microbial electrosynthesis systems for biogas production. Int J Hydrogen Energy 2019;44(48):26226–36.
[33] Rabaey K, Rozendal RA. Microbial electrosynthesis - revisiting the electrical route for microbial production. Nat Rev Microbiol 2010;8:706–16. https://doi.org/10.1038/nrmicro2422.
[34] Mei BA, Lau J, Lin T, Tolbert SH, Dunn BS, Pilon L. Physical interpretations of electrochemical impedance spectroscopy of redox active electrodes for electrical energy storage. J Phys Chem C 2018;122:24499–511. https://doi.org/10.1021/acs.jpcc.8b05241.
[35] Izadi P, Fontmorin JM, Godain A, Yu EH, Head IM. Parameters influencing the development of highly conductive and efficient biofilm during microbial electrosynthesis: the importance of applied potential and inorganic carbon source. npj Biofilms Microbiomes 2020;6:1–15. https://doi.org/10.1038/s41522-020-00151-x.
[36] Siegert M, Yates MD, Spormann AM, Logan BE. Methanobacterium dominates biocathodic archaeal communities in methanogenic microbial electrolysis cells. ACS Sustainable Chem Eng 2015;3:1668–76. https://doi.org/10.1021/acssuschemeng.5b00367.
[37] Blasco-Gómez R, Batlle-Vilanova P, Villano M, Balaguer M, Colprim J, Puig S. On the edge of research and technological application: A critical review of electromethanogenesis. Int J Mol Sci 2017;18(4):874.
[38] del Pilar Anzola Rojas M, Mateos R, Sotres A, Zaiat M, Gonzalez ER, Escapa A, et al. Microbial electrosynthesis (MES) from CO2 is resilient to fluctuations in renewable energy supply. Energy Convers Manage 2018;177:272–9.
[39] Mateos R, Sotres A, Alonso RM, Escapa A, Morán A. Impact of the start-up process on the microbial communities in biocathodes for electrosynthesis. Bioelectrochemistry 2018;121:27–37. https://doi.org/10.1016/j.bioelechem.2018.01.002.
[40] Ragab A, Katuri KP, Ali M, Saikaly PE. Evidence of spatial homogeneity in an electromethanogenic cathodic microbial community. Front Microbiol 2019;10. https://doi.org/10.3389/fmicb.2019.01747.
[41] Flores-Rodriguez C, Min B. Enrichment of specific microbial communities by optimum applied voltages for enhanced methane production by microbial electrosynthesis in anaerobic digestion. Bioresour Technol 2020;300:122624. https://doi.org/10.1016/j.biortech.2019.122624.
[42] Guo J, Peng Y, Ni BJ, Han X, Fan L, Yuan Z. Dissecting microbial community structure and methane-producing pathways of a full-scale anaerobic reactor digesting activated sludge from wastewater treatment by metagenomic sequencing. Microb Cell Fact 2015;14:33. https://doi.org/10.1186/s12934-015-0218-4.
[43] Shehab N, Li D, Amy GL, Logan BE, Saikaly PE. Characterization of bacterial and archaeal communities in air-cathode microbial fuel cells, open circuit and sealed-off reactors. Appl Microbiol Biotechnol 2013;97:9885–95. https://doi.org/10.1007/s00253-013-5025-4.
[44] Kobayashi H, Saito N, Fu Q, Kawaguchi H, Vilcaez J, Wakayama T, et al. Bio-electrochemical property and phylogenetic diversity of microbial communities associated with bioelectrodes of an electromethanogenic reactor. J Biosci Bioeng 2013;116(1):114–7.